iScience

CellPress

Article

Cell Cycle Progression Determines Wing Morph in the Polyphenic Insect *Nilaparvata lugens*

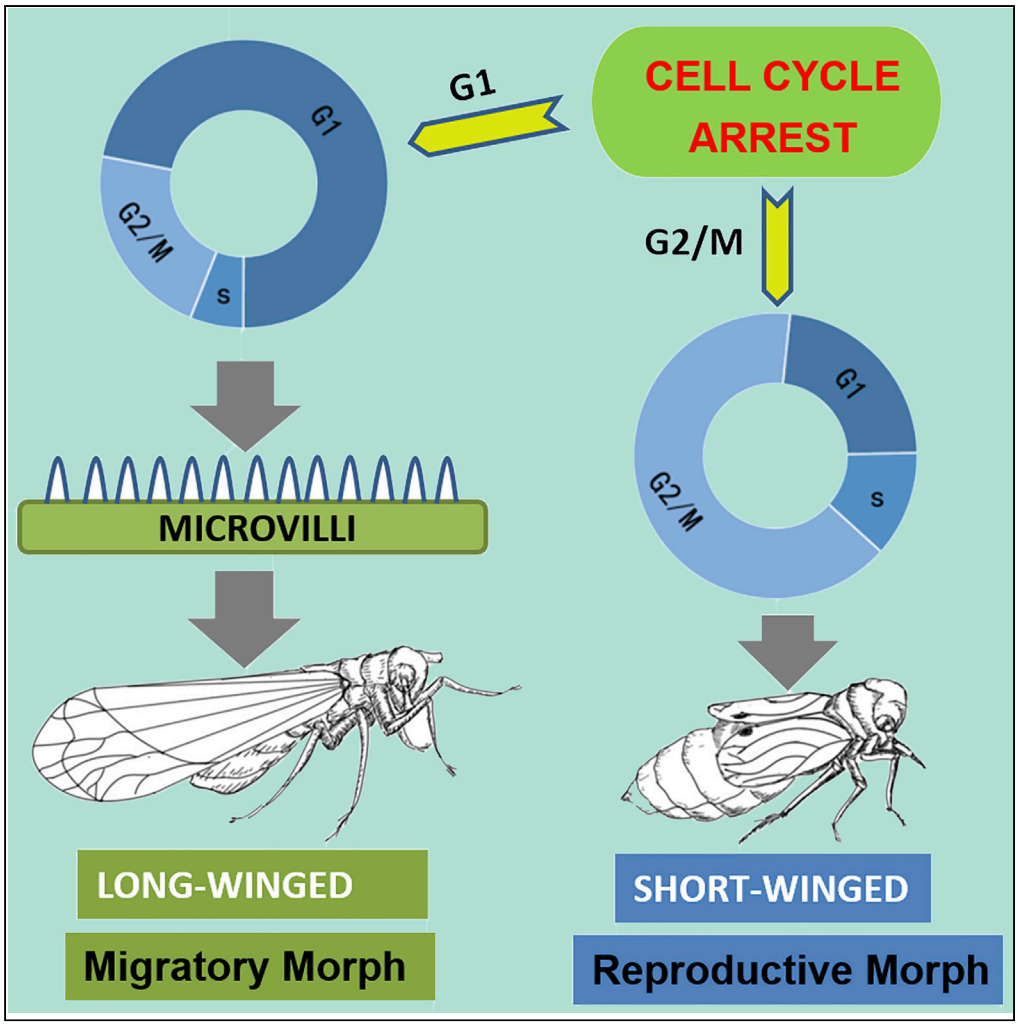

Xinda Lin, Han Gao, Yili Xu, Yuwei Zhang, Yan Li, Mark D. Lavine, Laura Corley Lavine

linxinda@cjlu.edu.cn

HIGHLIGHTS

Genes important in determining cell numbers are necessary to form long wings

Long-winged development was characterized by microvilli-like structures

Cells of adult short wing pads are largely in the G2/M phase of the cell cycle

Cells of adult long wing pads are largely in the G1 phase of the cell cycle

Lin et al., iScience *23*, 101040
April 24, 2020
https://doi.org/10.1016/j.isci.2020.101040

iScience

CellPress

Article

Cell Cycle Progression Determines Wing Morph in the Polyphenic Insect *Nilaparvata lugens*

Xinda Lin,[1,3,*] Han Gao,[1] Yili Xu,[1] Yuwei Zhang,[1] Yan Li,[1] Mark D. Lavine,[2] and Laura Corley Lavine[2]

SUMMARY

Wing polyphenism is a phenomenon in which one genotype can produce two or more distinct wing phenotypes adapted to the particular environment. What remains unknown is how wing pad development is controlled downstream of endocrine signals such as insulin and JNK pathways. We show that genes important in cellular proliferation, cytokinesis, and cell cycle progression are necessary for growth and development of long wings. Wing pad cellular development of the long-winged morph was characterized by a highly structured epithelial layer with microvilli-like structures. Cells of adult short wing pads are largely in the G2/M phase of the cell cycle, whereas those of long wings are largely in G1. Our study is the first to report the comparative developmental and cellular morphology and structure of the wing morphs and to undertake a comprehensive evaluation of the cell cycle genes necessary for wing development of this unique, adaptive life history strategy.

INTRODUCTION

Wing polyphenism is a phenomenon in which one genotype can produce two or more distinct wing phenotypes, which enables insects, such as aphids, crickets and ants, to adapt to environmental changes (Abouheif and Wray, 2002; Brisson, 2010; Zera and Denno, 1997; Zera and Harshman, 2001; Zera et al., 1998). Environmental factors that are shown to influence wing morph are nymphal crowding, nutrition, and wounding (Denno and Roderick, 1990; Kisimoto, 1956, 1965). The brown planthopper (*Nilaparvata lugens*) is a well-studied insect pest that develops short wings when environmental quality is high but develops long wings and migrates away when food quality is low. Endocrine regulation, which is tightly coordinated with both whole animal circulating signals such as nutrition and cellular signaling pathways, is a major regulator of environmentally induced wing polyphenisms in insects (Lin and Lavine, 2018; Zera et al., 2007; Zera, 2003; Zera and Tiebel, 1988). Ectopic application of the insect endocrine hormone, juvenile hormone (JH) and the JH antagonist precocene, have been reported to affect brown planthopper wing-form development (Ayoade et al., 1996; Bertuso and Tojo, 2002). Similar effects of ectopic JH application were also observed in the cricket *Gryllus rubens* (Zera and Tiebel, 1988) and aphid *Aphis fabae* (Hardie, 1981) indicating that endocrine regulation of wing growth proximately controls adaptive wing phenotypes. Recently, we showed, for the first time, that glucose concentration of the host plant regulates wing morph development in the brown planthopper (Lin et al., 2018). This was the first report of the crucial link between host plant quality and the adaptive phenotype of the insect. What we have found is that translation of the environmental factors into a long-winged (macropterous) or a short-winged (brachypterous) phenotype requires an intricate and complex coordination of whole-organism signals with developmental and cellular processes during growth and development (Lin and Lavine, 2018; Lin et al., 2018).

Endocrine regulation, which is tightly coordinated with cellular signaling pathways regulating growth and development, is critical in wing polyphenisms (Lin and Lavine, 2018; Zera et al., 2007; Zera, 2003; Zera and Tiebel, 1988). In brown planthoppers, JNK signaling (Lin et al., 2016a) and the insulin signaling pathway (Lin et al., 2016b; Xu et al., 2015) have been shown to be required for mediating wing development. The transcription factor FOXO, a key regulator of the insulin signaling pathway, controls cell growth and regulates *Drosophila* organ size by controlling cell proliferation (Puig et al., 2003). In the brown planthopper normal insulin signaling results in long-winged morphs, apparently through its inhibition of FOXO, whereas interruption of insulin signaling, such as by activation of the insulin receptor 2 gene, allows FOXO activation and results in short-winged morphs (Lin et al., 2016b; Xu et al., 2015). In addition, wounding of the nymphal brown planthopper results in upregulation of FOXO, also resulting in short-winged morph formation (Lin et al., 2016c). There is evidence that insulin signaling also mediates wing polyphenism in the soapberry bug *Jadera haematoloma*, suggesting that this pathway may have been independently co-opted as a developmental mechanism for polyphenism across divergent taxa.

[1]Key Laboratory of Marine Food Quality and Hazard Controlling Technology of Zhejiang Province, College of Life Sciences, China Jiliang University, Hangzhou 310018, China

[2]Department of Entomology, Washington State University, Pullman, WA 99164-6382, USA

[3]Lead Contact

*Correspondence: linxinda@cjlu.edu.cn

https://doi.org/10.1016/j.isci.2020.101040

What remains unknown is how insulin signaling/FOXO direct changes in morphology during wing morph development to result in the appropriate adaptive phenotype. In a hemimetabolous insect like the brown planthopper, wing morphogenesis proceeds from nymphal structures called wing pads. The wing pads' integument consists of a single layer of epidermal cells. After ecdysis, the flat and thin epidermal cells of the wing pad become columnar. The structural changes are a result of epidermal cell divisions (Rauschenbach et al., 2012; Riddiford, 2012). The cells increase in number, with the appearance of more numerous mitotic divisions after the previous ecdysis (Riddiford, 2012). Here we investigated the cellular mechanisms of wing polyphenism in the brown planthopper, which has the most comprehensive and detailed physiological and genetic mechanisms studied to date underlying its wing polyphenism. We found that activation of insulin signaling in the last two nymphal instars resulted in specific changes of cell morphology and proliferation in nymphal wing pads that resulted in long-winged adults. Conversely, inhibition of insulin signaling in the final two nymphal instars resulted in inhibition of cell cycle progression in wing pads, and the resulting adults retained their non-functional (i.e., short) wing morphology.

RESULTS

Long Wing Pads Exhibit Increased and Regular Microvilli-like Structures

We investigated whether there were ultrastructural differences between the wing pads of nymphs fated to become long winged versus those fated to become short winged. Unfortunately, there is no reliable marker in nymphs to identify their wing fate, and the removal of a single wing bud from a nymph causes the remaining wing bud to develop into a short wing (this is because injury affects wing morph determination, see Lin et al., 2016a, 2016b, 2016c). However, we took advantage of the role of the insulin signaling pathway in wing morph determination to artificially manipulate the wing morph, and then to correlate this with potential differences in wing bud ultrastructure. RNAi-mediated down-regulation of the transcription factor *FOXO* in fourth-instar nymphs results in a complete developmental switch to long-winged adults (Lin et al., 2016b; Xu et al., 2015). Conversely, RNAi-mediated down-regulation of the insulin receptor *InR1* in fourth-instar nymphs results in a nearly complete developmental switch to short-winged adults (Xu et al., 2015). Thus, we compared the ultrastructure of wing pads dissected from fifth-instar nymphs (95 h post-molt) that had been injected in the previous instar with either *FOXO* dsRNA to induce long wings or *InR1* dsRNA to induce short wings (Transparent Methods, Tables S1, S2, and Figure 1). We found that the outer surface of the cells on the margin of the wing pads from *FOXO* dsRNA-injected nymphs all contained orderly and regular microvilli-like structures of the epithelial layer (Transparent Methods and Figure 1). These microvilli-like structures were observed in some wing pads taken from non-treated control nymphs (which can develop into either morph) but were never observed in wing pads taken from *InR1* dsRNA-injected nymphs (i.e., short-winged nymphs).

After noting the presence of the microvilli-like structures on the wing bud cells of fifth-instar nymphs fated to become long-winged adults, we more closely examined the morphology of those cells over the course of the fifth instar. We compared the margins of the wing bud in *FOXO* and *InR1* dsRNA-injected nymphs at eight time points beginning 75 h after eclosion to the fifth instar (Transparent Methods and Figure 2). At 75 h, cellularization of the wing bud had not started, and no microvilli-like structures were visible, although in long-winged (i.e., *FOXO* knockdown) nymphs there were aggregations of actin at the border of the wing pads (Figure 2). By 78 h, cellularization was initiated and the microvilli-like structures could be observed on the cell surface from long-wing morph pads (Figure 2). These epithelial furrows continued to grow at 81 h and 84 h, and by 90 h most appeared to be fully developed. The complex, microvilli-like structures remained visible until eclosion. Again, we observed no obvious microvilli-like structures in wing pads from the short-winged nymphs, although we did observe that the margins of these cells became more irregular and that microvilli-like structures formed between some cells during wing bud development (Figure 2). Thus the wing pads of nymphs fated to be long winged can be reliably distinguished from those fated to be short winged through the presence of microvilli-like structures on the outer layer of epithelial cells in the wing pads of the long-winged nymphs.

The Cell Cycle Is Arrested at Different Phases in Long and Short Wings

Given the cellular differences in wing pads developing into long or short wings, we examined whether there were any differences in the cells of adult wings. We collected long and short wings of newly eclosed brown planthopper adults, dissociated the cells, and analyzed the cells using flow cytometry. Analysis of DNA content showed that the cells of long and short wings were arrested at distinct cell cycle phases (Transparent Methods and Figure 3). Most of the cells from long wings were arrested at the G1 phase (72.4%, Figure 3B

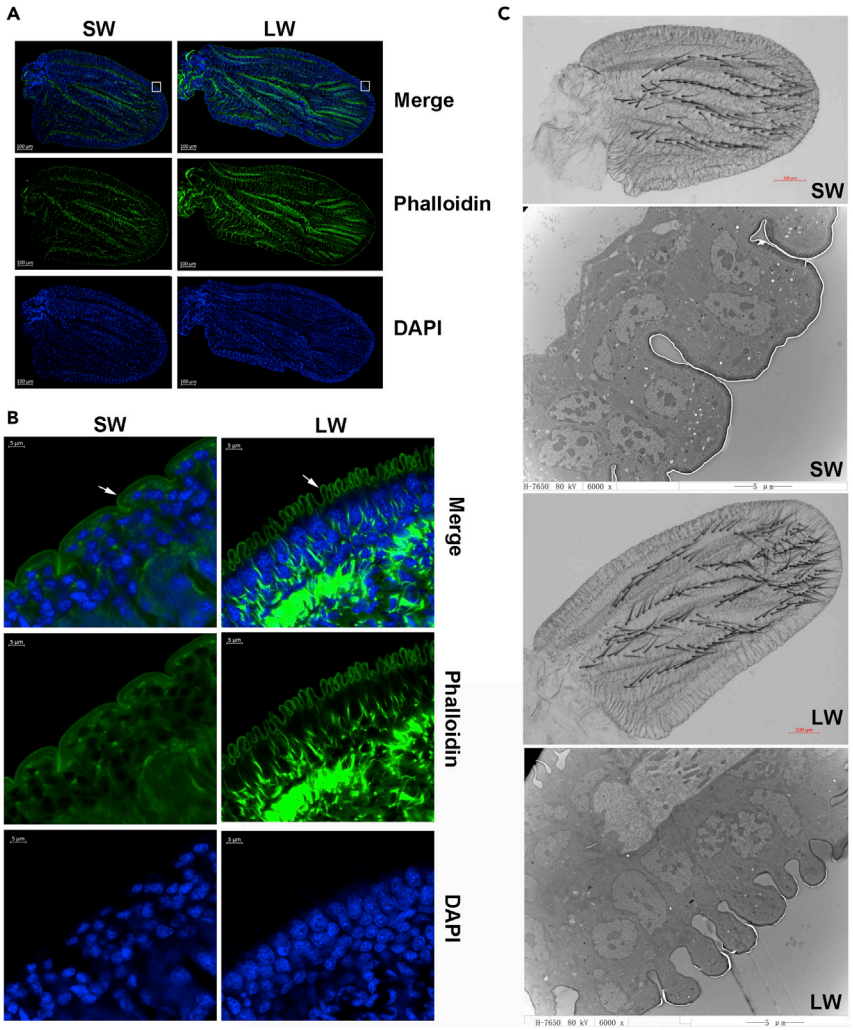

Figure 1. Differences in Ultrastructure of Wing Pads Developing into Short or Long Brown Planthopper Wings

(A and B) (A) Whole wing pads were dissected 95 h post-molt to fifth instar, and actin stained with phalloidin-iFluor 488 (green) and nuclei stained with DAPI (blue). White rectangles indicate regions that are further magnified in (B). (B) Enlargement of (A) showing the distal portion of the wing pad with the microvilli-like epithelium in long-winged individuals; arrows indicate the differential structures in the long and short wings.

(C) Transmission electron microscopic image of the wing pads of the fifth-instar nymphs (6000X). SW, short-winged development induced by knockdown of *InR1*; LW, long-winged induced by knockdown of *FOXO*.

and 3C), which suggests that these cells have already undergone mitosis. The majority of cells from short wings were arrested in the G2/M phase (65.0%, Figure 3B and 3C), which suggests that these adult cells had undergone DNA replication but not cell division.

Interfering with Cell Division in Late Instar Nymphs Prevents the Development of Long-Winged Adults

Given the inherent size differences between long and short wings, we sought to confirm that formation of long wings requires higher rates of cellular proliferation. We tested this by down-regulating a suite of highly conserved genes known to regulate the cell cycle: members of the E2F/DP family transcription factors (*E2F3*, *E2F5*, *E2F6*, *E2F7*, *E2F8*, *DP1*, *DP2*) (Trimarchi and Lees, 2002), as well as *cyclin E1* (*CCNE*) and the cyclin-dependent kinases *CDK1* and *CDK2* (Malumbres and Barbacid, 2005). We therefore hypothesized that if we down-regulated these cell cycle regulatory genes through RNAi, cellular proliferation would probably be reduced, which would inhibit development of the long-winged form. Indeed, down-regulation of all the cell-cycle regulatory genes, by injection of the appropriate dsRNA into fourth-instar nymphs, led

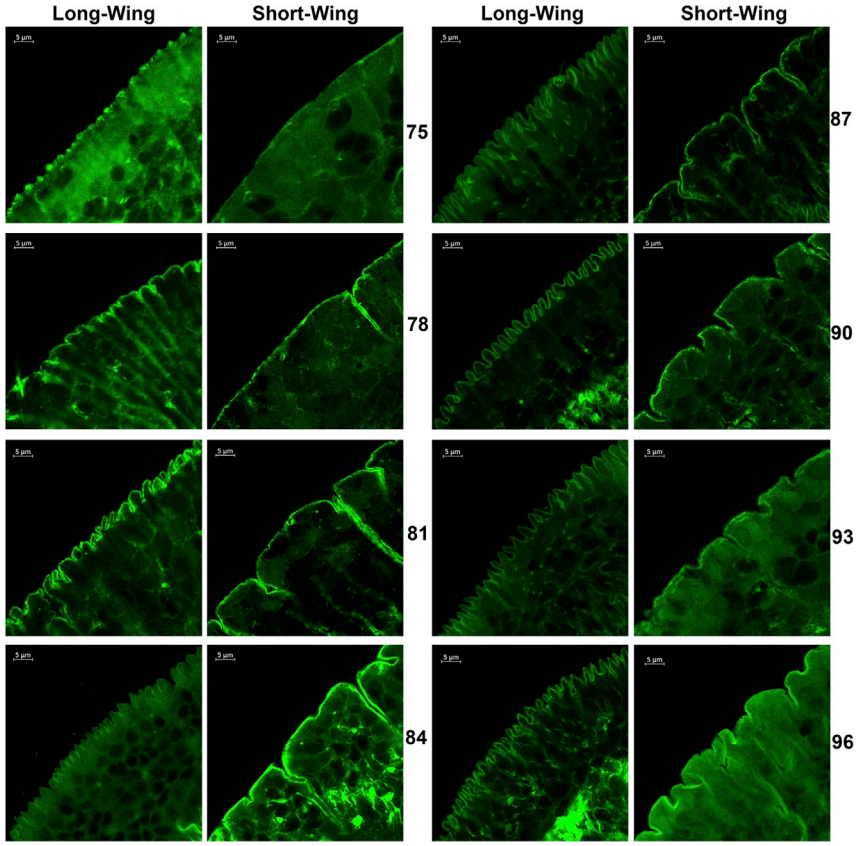

Figure 2. Time Course of Development of Wing Pad Epithelium in Long versus Short Brown Planthopper Wings

Long-wing or short-wing development was induced by knockdown of *InR1*(short wings) or *FOXO* (long wings) in the fourth nymphal instar. Wing buds were dissected and stained with phalloidin-iFluor 488 (green) at the indicated time in hours after eclosion of the fifth-instar nymph. Scale bar, 5μm.

to a significant decrease in the percentage of long-winged adults for both females and males compared with controls (Transparent Methods and Figures 4A and 4B).

Interfering with cytoskeletal dynamics, which are also required for cell division (Wu et al., 2012), also prevented the development of long-winged adults. RNAi-mediated down-regulation of the microtubule-associated protein Futsch and the actin-organizing cadherin PCDH15 in fifth-instar nymphs resulted in significant decreases in the percentage of long-winged adult males and females (Transparent Methods and Figures 5A and 5B). Likewise, injection of the microtubule disruptors paclitaxel and nocodazole into fifth-instar nymphs caused significant decreases in the percentage of long-winged adults relative to controls (Figures 5A and 5B). Fifth-instar nymphs were used in the experiments disrupting cytoskeletal dynamics because of a high degree of lethality in fourth-instar nymphs. Both long and short wings developing after RNAi or drug treatment are morphologically the same as natural (i.e., control) long and short wings, respectively (Figures S1 and S2).

Thus, active cellular division in the penultimate and ultimate nymphal instars is required for formation of long wings.

Wing Pads Developing into Long Wings Have More Nuclei/Area Than Those Developing into Short Wings

We used the correlation between the presence of microvilli-like structures in wing pads developing into long wings to differentiate short versus long wing pads in fifth-instar nymphs. We then compared the number of nuclei per given area (in this case 475 μm^2) from wing pads developing into long versus short wings. Those developing into long wings had a significantly higher number of nuclei/area than those developing

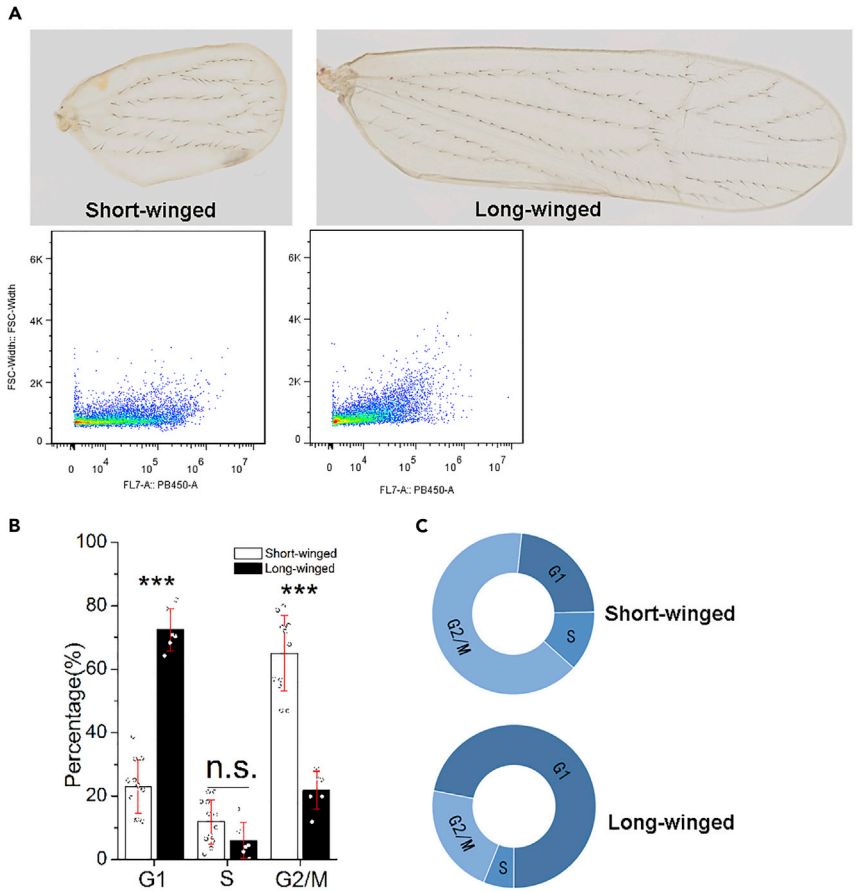

Figure 3. The Cell Cycle Is Arrested at Different Stages in Short and Long Brown Planthopper Wings

Flow cytometry was used to determine the cell cycle of dissociated cells from short and long wings from brown planthopper adults.

(A–C) (A) representative images of short and long wings from newly emerged adults; (B) percentages of cells in G1 and G2/M differed significantly between cells from short (n = 10) and long wings (n = 6). Student's t test range-test was used for statistical comparison. n.s., not significant; ***p < 0.001. Data are represented as mean ± SD; (C) Graph illustrating the distribution of cells in each phase of the cell cycle from short and long wings.

into short wings (Transparent Methods and Figure 6). This was true whether wings were developing naturally (i.e., no treatment or dsGFP-injected) or whether they were induced to be short (by RNAi-mediated knockdown of the cell cycle or cytoskeletal regulatory genes or use of microtubule disruptors, as in the previous section) or long (knockdown of *FOXO*). This is another indication that the wing pads of nymphs developing into long-winged adults are more mitotically active than those developing into short-winged adults.

We used RT-PCR to measure the expression of genes after down-regulation by RNAi. The result showed that the expressions of all the genes we down-regulated by RNAi were reduced significantly (Transparent Methods and Figure S3).

Injection of Paclitaxel Reverses *FOXO* dsRNAi Phenotype

FOXO limits microtubule stability and regulates microtubule organization (Tarver et al., 2012; Tibbetts et al., 2013). Paclitaxel is a drug used against several solid tumors targeting tubulin, mainly via suppressing microtubule dynamics during mitotic spindle assembly in cells undergoing division (Suren-Castillo et al., 2012). We used paclitaxel to test the effect of interfering with microtubule dynamics in nymphs that had been injected with *FOXO* dsRNA. Normally dsRNA-mediated knockdown of *FOXO* in fourth-instar nymphs results in 100% development of long-winged adults. However, when these *FOXO*-knockdown nymphs were subsequently injected with paclitaxel in the fifth instar, the majority of nymphs developed into

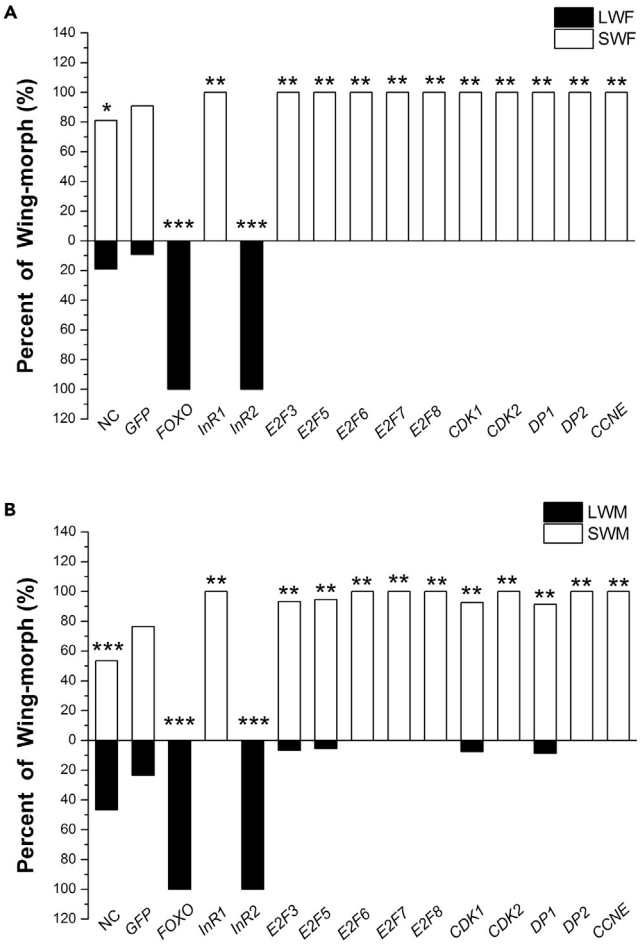

Figure 4. RNAi-Mediated Down-regulation of Cell Cycle Regulatory Genes in Fourth-Instar Nymphs Decreased the Ratio of Long-Winged Adult Brown Planthoppers.

(A) Females and (B) males.

Statistical comparisons to the dsGFP-injected nymphs were made using chi-square test. *$p < 0.05$, **$p < 0.01$, ***$p < 0.001$. SWF, short-winged female; SWM, short-winged male; LWF, long-winged female; LWM, long -winged male. NC (non-injected controls) (n = 159 females, 156 males), dsGFP (n = 98 females, 98 males), dsFOXO (n = 72 females, 63 males), dsInR1 (n = 65 females, 59 males), dsInR2 (n = 94 females, 74 males), dsE2F3 (n = 123 females, 112 males), dsE2F5 (n = 74 females, 52 males), dsE2F6 (n = 62 females, 74 males), dsE2F7 (n = 52 females, 63 males), dsE2F8 (n = 64 females, 67 males), dsCDK1 (n = 55 females, 62 males), dsCDK2 (n = 115 females, 104 males), dsDP1 (n = 61 females, 69 males), dsDP2 (n = 70 females, 60 males), dsCCNE (n = 52 females, 44 males).

short-winged adults (Transparent Methods, Tables S1, S2, and Figure 7A). Although the phenotypic reversal was not complete (some nymphs still developed long wings), this indicates that the effects of paclitaxel are downstream of the effects of dsFOXO on wing development.

Having confirmed that cellular proliferation must occur in the wing pads of nymphs for them to become long winged, we also examined the effects of *FOXO* knockdown on the transcription of a number of genes mediating cell division (Transparent Methods, Tables S3–S5 and Figure 7B). We found that wing pads from nymphs injected with dsFOXO showed significantly greater amounts of transcription of the cell-cycle regulatory genes *E2F3*, *E2F5*, *E2F6*, *E2F7*, *E2F8*, *CDK1*, *CDK2*, *DP1*, *DP2*, and *CCNE* and the cytoskeletal regulating genes *Futsch* and *PCDH15* than wing pads from dsGFP-injected controls. Furthermore, in nymphs that were injected with dsFOXO followed by paclitaxel as mentioned earlier, transcripts of all these genes returned to control levels. Thus, down-regulation of *FOXO* results in the transcriptional activation of an array of genes required for cell division, but interference of cell division through the action of paclitaxel reverses this process.

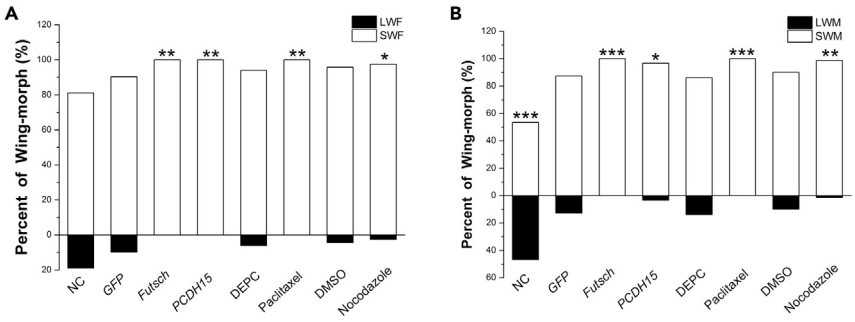

Figure 5. Cytoskeletal Dynamics Are Required in Fifth-Instar Nymphs for the Development of Long-Winged Adult Brown Planthoppers.

(A) Females and (B) males.

dsRNA of *PCDH15* and *Futsch*, or the microtubule inhibitors nocodazole and paclitaxel, were injected into fifth-instar nymphs. *PCDH15*, *Futsch*, and NC (non-injected) treatments were compared with dsGFP-injected treatment by chi-square test; paclitaxel injections were compared with diethyl pyrocarbonate (DEPC)-treated water (solvent) injections by chi-square test; nocodazole injections were compared with DMSO (solvent) injections by chi-square test. *$p < 0.05$, **$p < 0.01$, ***$p < 0.001$. SWF, short-winged female; SWM, short-winged male; LWF, long-winged female; LWM, long-winged male. NC (n = 164 females, 161 males), dsGFP (n = 103 females, 55 males), dsFutsch (n = 68 females, 71 males), dsPCDH15 (n = 55 females, 59 males), diethyl pyrocarbonate (DEPC)-treated water (n = 83 females, 108 males), DMSO (n = 94 females, 121 males), nocodazole (n = 80 females, 74 males), paclitaxel (n = 84 females, 64 males).

These experiments, taken together, characterize for the first time the morphological, structural, and cellular differences between the long-winged brown planthopper and the so-called short-winged morph. The long-winged morph has a typical wing that proliferates and grows into its adult form during the last nymphal instar as the nymphal wing pads of hemimetabolous insects are known to do. The so-called short-winged or brachypterous morph, however, can be characterized based on morphological, structural, and cellular data to be equivalent to the undifferentiated wing bud of late instar nymphs, and the cells have been arrested before cell division occurs.

DISCUSSION

Wing development in the adult brown planthopper is determined by the dietary sugar content of the rice plants the insects feed on as immatures (Lin et al., 2018). High levels of dietary glucose in senescing rice plants serve as a signal that leads to the development of the long-winged, flight-capable adult, which flies away from the old host plants to find new food sources (Lin et al., 2018). Lower levels of dietary glucose in rice plants that are developing result in short-winged brown planthoppers that are not able to fly. Previous research has shown that the insulin signaling pathway mediates wing morph fate through the transcription factor FOXO, which when activated inhibits wing cell growth and results in the development of the short-winged morph (Lin et al., 2016b; Xu et al., 2015). It is not yet clear how FOXO specifically suppresses cell division in wing pads or what genes become active when FOXO is inactivated that promote growth of the wings. What is clear is that the development of long wings requires active cellular division in the final nymphal instars, and thus the activation of the insulin signaling pathway, through inactivation of FOXO, in combination with other regulatory factors, such as DPP in regulating wing venation (Shin et al., 2012), ultimately results in cellular proliferation in the nymphal wing pads.

When we compared the wing pads of nymphs developing into long-winged adults with those developing into short-winged adults, there was a striking difference in the morphology of the distal epithelial cells. These cells in the pads from developing long wings contained numerous and complex 3D epithelial furrows, which is very different from typical holometabolous wing development (Diaz de la Loza and Thompson, 2017). Hemimetabolous wings, like those of brown planthoppers, develop as cuticle-encased external pads, and most of the growth occurs in the ultimate nymphal state (Erezyilmaz et al., 2006). Although we do not know the precise function of the microvillar projections we see in the wing pads of brown planthoppers, we speculate that the microvilli-like structures are necessary due to the rapid growth and proliferation of the much larger adult wings under the last instar nymphal cuticular wing pad in the long-winged morph, whereas the absence of these structures in the short-winged morph is because there is a relative low rate of cell growth or proliferation. In addition, the presence or absence of these microvilli-like structures

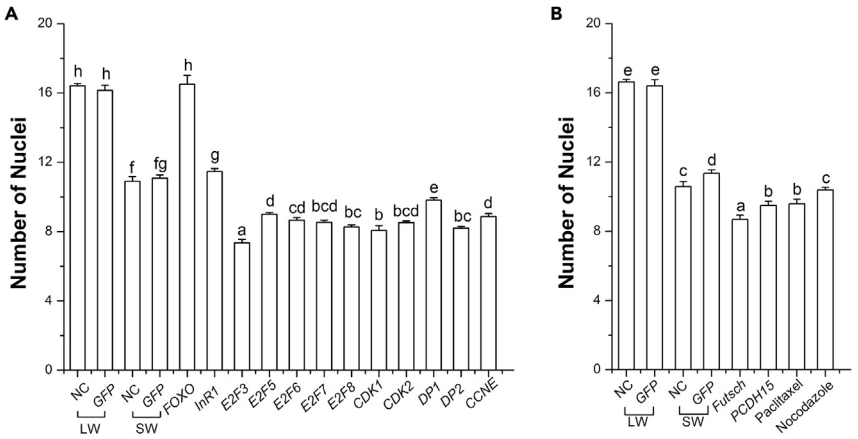

Figure 6. The Number of Nuclei Per Area Is Greater in Long Than in Short Brown Planthopper Wings

Wings were dissected from adults 1 h after eclosion. Nuclei were stained with DAPI, and the number of nuclei per 475 μm^2 area was counted. LW, long-winged adults; SW, short-winged adults. Data are represented as mean ± SD.

In (A), all experimental treatments were performed in fourth-instar nymphs. NC, non-treated control (n = 32 for LW and n = 31 for SW); GFP, dsGFP-injected control (n = 35 for LW and n = 34 for SW). Other treatments are the same as those in Figures 1 and 2: dsRNA injections of FOXO (n = 49), *InR1* (n = 40), *E2F3* (n = 40), *E2F5* (n = 44), *E2F6* (n = 45), *E2F7* (n = 44), *E2F8* (n = 42), *CDK1* (n = 45), *CDK2* (n = 50), *DP1* (n = 43), *DP2* (n = 44), *CCNE* (n = 36).

In (B), all experimental treatments were performed in fifth-instar nymphs, NC, non-treated control (n = 33 for LW and n = 33 for SW); GFP, dsGFP-injected control (n = 35 for LW and n = 35 for SW), *Futsch* (n = 33), and *PCDH15* (n = 30), and injection of microtubule inhibitors paclitaxel (n = 47) and nocodazole (n = 47). All these treatments produce short-winged adults, whereas injection of ds*FOXO* produces long-winged adults. Comparisons of number of nuclei per treatment were by Duncan's multiple range-test. Significantly different treatments ($p < 0.05$) are indicated by different letters above bar.

serves as a morphological indicator useful for identifying nymphs as developing into long- or short-winged adults, something that was not previously discernible until adult emergence.

Our finding that cells in long-winged morphs tend to be in G_1 of the cell phase, whereas cells in short wings tend to be in G_2/M indicates that the cells in short-winged adults have been arrested before the onset or completion of cellular division. As morphologically the wing buds of adult short-winged brown planthoppers are the same as the wing pads of the terminal nymphal instar, we hypothesize that activated FOXO inhibits cell division just before the initial round of cell division in late instar wing buds. Thus, in long-winged brown planthoppers, wing development proceeds as it normally would in other winged hemimetabolous insects. The ancestral state for hemimetabolous insects is to grow two fully formed pairs of wings, and the brachypterous or short-winged adult form found in wing polyphenic insects such as the brown planthopper is an adaptive, derived condition. Our results indicate that when FOXO becomes activated through an increase in dietary sugar content, FOXO signaling inhibits cellular proliferation and leads to the arrest of the cells of the wing pads before they complete cellular division, resulting in the short, non-functional wings of adults. Although FOXO is an important protein in controlling wing form development, FOXO is unlikely the only downstream transcription factor that regulates cellular proliferation and wing development, as it is known from other insects such as *Drosophila* that wing development is regulated by a complex set of signaling pathways.

This model also presents a reasonable explanation for why in the brown planthopper and other wing polyphenic species, such as some field crickets, the sensitive period in which environmental signals can affect wing morph is found to be within the last one or two nymphal instars, with the specific time point varying with the species and type of environmental cue (Bertuso et al., 2002; Iwanaga and Sumino, 1986; Zera and Tiebel, 1988). This sensitive period may simply be the time in which wing pad cells begin proliferation to the adult wing. The suppression of growth in short-winged brown planthoppers also raises the question of how specificity is maintained for the wings, allowing other tissues to proliferate despite receiving the same environmental and physiological cues. The heterochrony in growth of the adult tissues during hemimetabolous post-embryonic development wherein most wing growth occurs in the terminal nymphal instar, whereas other structures grow incrementally over nymphal development (Erezyilmaz et al., 2006), would allow for the evolution of wing polyphenism in these species. Wing pads are especially sensitive to inhibition of

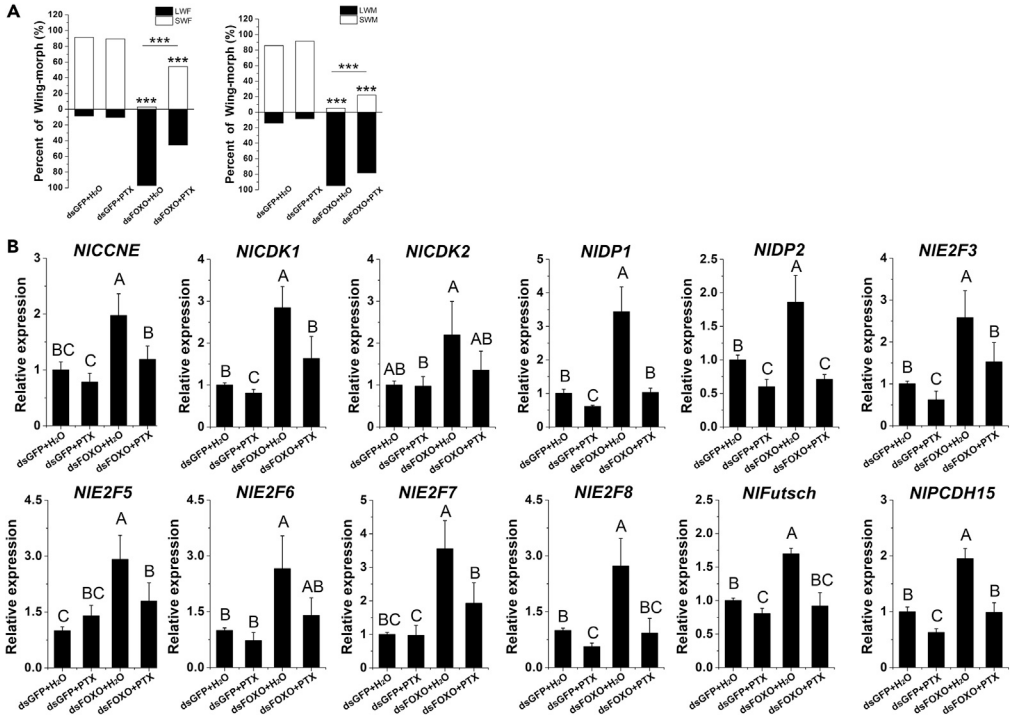

Figure 7. Effects on Wing Morph and Transcription of Cell Division-Related Genes After Injection of FOXO dsRNA and/or Paclitaxel

(A) Fourth-instar nymphs received injections of dsGFP or dsFOXO, followed by the second injection of paclitaxel (PTX) or water at the fifth-instar nymph stage. dsFOXO + PTX (n = 68 females, 43 males), dsFOXO + H2O (n = 37 females, 41 males), dsGFP + PTX (n = 31 females, 27 males), dsGFP + H2O (n = 32 females, 27 males).

(B) Fourth-instar nymphs received injections, wing buds were subsequently dissected, and relative expression of the genes *E2F3*, *E2F5*, *E2F6*, *E2F7*, *E2F8*, *CDK1*, *CDK2*, *DP1*, *DP2*, *CCNE*, *Futsch*, and *PCDH15* were measured by RT-PCR. Chi-square test was used in (A). ***$p < 0.001$. Twelve biological replicates were used for each treatment. Treatments found to be significantly different by Duncan's multiple range-test ($p < 0.05$) are indicated by different letters (B). Data are represented as mean ± SD.

See Table S4 and S5 for normality test.

cell division in the final nymphal instar because this is the point at which they do the entirety of their cellular division and proliferation into the adult wing structure, whereas other structures have nearly or fully attained their adult size already.

Our findings point to a model for wing polyphenism in which the wing pads are poised for cell division until a sensitive period late in nymphal development (Figure 8), when environmental signals are transduced to either allow cell division to proceed to the long-winged morph or block it at G_2/M, leaving the wing pad cells in a state of arrested development, resulting in the short-winged adult morph.

Limitations of the Study

We were not able to determine the efficiency of primers or to carry out the approach including quantitative standards.

METHODS

All methods can be found in the accompanying Transparent Methods supplemental file.

SUPPLEMENTAL INFORMATION

Supplemental Information can be found online at https://doi.org/10.1016/j.isci.2020.101040.

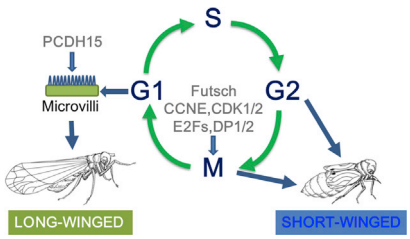

Figure 8. Model of Wing Polyphenism in the Brown Planthopper

Dietary glucose concentration above a threshold level activates the insulin signaling pathway, which represses the transcription factor FOXO. If the insulin signaling pathway is not activated, FOXO is active. FOXO directly or indirectly acts on cell cycle progression in wing pads: if FOXO is active cell-cycle progression is arrested (at G2/M) and short-winged adults develop. If FOXO is not active cell-cycle progression continues past G2/M, cells continue through multiple rounds of mitosis, and long-winged adults develop.

ACKNOWLEDGMENTS

This research was supported by the National Natural Science Foundation of China (31672023, 31471771, 31741107) and the Natural Science Foundation of Zhejiang Province (Key program, LZ20C140002) to X.L. and supported in part by the USDA National Institute of Food and Agriculture, Hatch project 1014918 to Laura Lavine.

AUTHOR CONTRIBUTIONS

X.L. conceived and designed the study, X.L., H.G., Y.X., Y.Z. and Y.L. performed experiment and analyzed data, X.L., L.C.L. and M.D.L. wrote the paper. All authors discussed the results and commented on the manuscript.

DECLARATION OF INTERESTS

The authors declare no competing interests.

Received: October 24, 2019
Revised: January 23, 2020
Accepted: April 1, 2020
Published: April 24, 2020

REFERENCES

Abouheif, E., and Wray, G.A. (2002). Evolution of the gene network underlying wing polyphenism in ants. Science *297*, 249–252.

Ayoade, O., Morooka, S., and Tojo, S. (1996). Metamorphosis and wing formation in the Brown plant hopper, Nilaparvata lugens, after topical application of precocene II. Arch. Insect Biochem. Physiol. *32*, 485–491.

Bertuso, A.G., Morooka, S., and Tojo, S. (2002). Sensitive periods for wing development and precocious metamorphosis after precocene treatment of the brown planthopper, Nilaparvata lugens. J. Insect Physiol. *48*, 221–229.

Bertuso, A.G., and Tojo, S. (2002). The nature and titer of juvenile hormone in the brown planthopper, Nilaparvata lugens(Homoptera: Delphacidae) in relation to wing morphogenesis and oocyte development. Appl. Entomol. Zool *37*, 117–125.

Brisson, J.A. (2010). Aphid wing dimorphisms: linking environmental and genetic control of trait variation. Philos. Trans. R. Soc. Lond. B Biol. Sci. *365*, 605–616.

Denno, R.F., and Roderick, G.K. (1990). Population biology of planthoppers. Annu. Rev. Entomol. *35*, 32.

Diaz de la Loza, M.C., and Thompson, B.J. (2017). Forces shaping the Drosophila wing. Mech. Dev. *144*, 23–32.

Erezyilmaz, D.F., Riddiford, L.M., and Truman, J.W. (2006). The pupal specifier broad directs progressive morphogenesis in a direct-developing insect. Proc. Natl. Acad. Sci. U S A *103*, 6925–6930.

Hardie, J. (1981). Juvenile hormone and photoperiodically controlled polymorphism in Aphis fabae : postnatal effects on presumptive gynoparae. J. Insect Physiol. *27*, 347–355.

Iwanaga, K., and Sumino, T. (1986). Effects of juvenile hormone and rearing density on wing dimorphism and oöcyte development in the brown planthopper, Nilaparvata lugens. J. Insect Physiol. *32*, 585–590.

Kisimoto, R. (1956). Effect of crowding during the larval period on the determination of the wing-form of an adult plant-hopper. Nature *178*, 641–642.

Kisimoto, R. (1965). Studies on polymorphism and its role playing in the population growth of brown planthopper , Nilaparvata lugens (Stal). Bull. Shikoku Agric. Exp. Stn *13*, 101–106.

Lin, X., and Lavine, L.C. (2018). Endocrine regulation of a dispersal polymorphism in winged insects: a short review. Curr. Opin. Insect Sci. *25*, 20–24.

Lin, X., Xu, Y., Jiang, J., Lavine, M., and Lavine, L.C. (2018). Host quality induces phenotypic plasticity in a wing polyphenic insect. Proc. Natl. Acad. Sci. U S A *115*, 7563–7568.

Lin, X., Xu, Y., Yao, Y., Wang, B., Lavine, M.D., and Lavine, L.C. (2016a). JNK signaling mediates wing form polymorphism in brown planthoppers (Nilaparvata lugens). Insect Biochem. Mol. Biol. *73*, 55–61.

Lin, X., Yao, Y., Wang, B., Emlen, D.J., and Lavine, L.C. (2016b). Ecological trade-offs between migration and reproduction are mediated by the

nutrition-sensitive insulin-signaling pathway. Int. J. Biol. Sci. *12*, 607–616.

Lin, X., Yao, Y., Wang, B., Lavine, M.D., and Lavine, L.C. (2016c). FOXO links wing form polyphenism and wound healing in the brown planthopper, Nilaparvata lugens. Insect Biochem. Mol. Biol. *70*, 24–31.

Malumbres, M., and Barbacid, M. (2005). Mammalian cyclin-dependent kinases. Trends Biochem. Sci. *30*, 630–641.

Puig, O., Marr, M.T., Ruhf, M.L., and Tjian, R. (2003). Control of cell number by Drosophila FOXO: downstream and feedback regulation of the insulin receptor pathway. Genes Dev. *17*, 2006–2020.

Rauschenbach, I.Y., Laukhina, O.V., Alekseev, A.A., Adonyeva, N.V., Bogomolova, E.V., and Gruntenko, N.E. (2012). Dopamine effect on 20-hydroxyecdysone level is mediated by juvenile hormone in Drosophila females. Dokl Biochem. Biophys. *446*, 263–265.

Riddiford, L.M. (2012). How does juvenile hormone control insect metamorphosis and reproduction? Gen. Comp. Endocrinol. *179*, 477–484.

Shin, S.W., Zou, Z., Saha, T.T., and Raikhel, A.S. (2012). bHLH-PAS heterodimer of methoprene-tolerant and Cycle mediates circadian expression of juvenile hormone-induced mosquito genes. Proc. Natl. Acad. Sci. U S A *109*, 16576–16581.

Suren-Castillo, S., Abrisqueta, M., and Maestro, J.L. (2012). FoxO inhibits juvenile hormone biosynthesis and vitellogenin production in the German cockroach. Insect Biochem. Mol. Biol. *42*, 491–498.

Tarver, M.R., Coy, M.R., and Scharf, M.E. (2012). Cyp15F1: a novel cytochrome P450 gene linked to juvenile hormone-dependent caste differentiation in the termite Reticulitermes flavipes. Arch. Insect Biochem. Physiol. *80*, 92–108.

Tibbetts, E.A., Mettler, A., and Donajkowski, K. (2013). Nutrition-dependent fertility response to juvenile hormone in non-social Euodynerus foraminatus wasps and the evolutionary origin of sociality. J. Insect Physiol. *59*, 339–344.

Trimarchi, J.M., and Lees, J.A. (2002). Sibling rivalry in the E2F family. Nat. Rev. Mol. Cell Biol. *3*, 11–20.

Wu, W.J., Wang, Y., Huang, H.J., Bao, Y.Y., and Zhang, C.X. (2012). Ecdysone receptor controls wing morphogenesis and melanization during rice planthopper metamorphosis. J. Insect Physiol. *58*, 420–426.

Xu, H.J., Xue, J., Lu, B., Zhang, X.C., Zhuo, J.C., He, S.F., Ma, X.F., Jiang, Y.Q., Fan, H.W., Xu, J.Y., et al. (2015). Two insulin receptors determine alternative wing morphs in planthoppers. Nature *519*, 464–467.

Zera, A., Zhao, Z., and Kaliseck, K. (2007). Hormones in the field: evolutionary endocrinology of juvenile hormone and ecdysteroids in field Populations of the wing-dimorphic cricket Gryllus firmus. Physio Biochem. Zool. *80*, 592–606.

Zera, A.J. (2003). The endocrine regulation of wing polymorphism in insects: state of the art, recent surprises, and future directions. Integr. Comp. Biol. *43*, 607–616.

Zera, A.J., and Denno, R.F. (1997). Physiology and ecology of dispersal polymorphism in insects. Annu. Rev. Entomol. *42*, 207–230.

Zera, A.J., and Harshman, L.G. (2001). The physiology of life history trade-offs in animals. Annu. Rev. Ecol. Syst. *32*, 95–126.

Zera, A.J., Kobus, K., and Potts, J. (1998). The physiology of life-history trade-offs: experimental analysis of a hormonally induced life-history trade-off in Gryllus assimilis. Am. Nat. *152*, 7–23.

Zera, A.J., and Tiebel, K.C. (1988). Brachypterizing effect of group rearing, juvenile hormone III and methoprene in the wing-dimorphic cricket, Gryllus rubens. J. Insect Physiol. *34*, 489–498.

iScience, Volume *23*

Supplemental Information

Cell Cycle Progression Determines Wing Morph in the Polyphenic Insect *Nilaparvata lugens*

Xinda Lin, Han Gao, Yili Xu, Yuwei Zhang, Yan Li, Mark D. Lavine, and Laura Corley Lavine

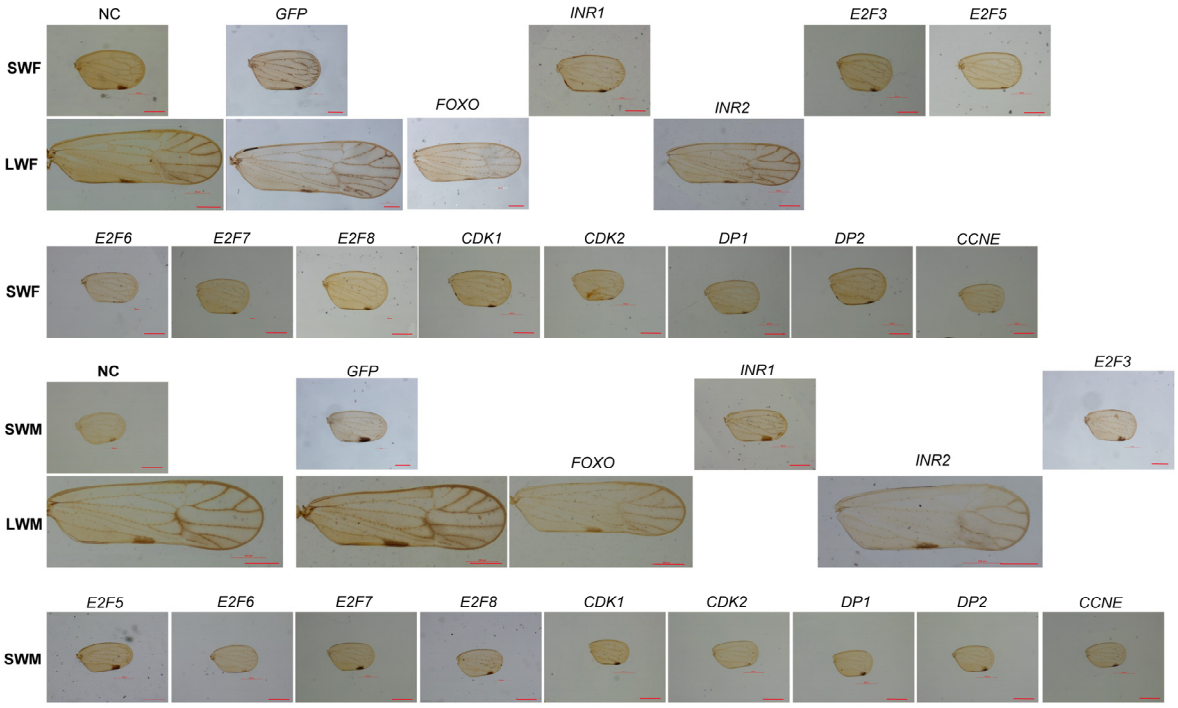

Figure S1: Representative long and short wings after treatment at the 4th instar nymph stage, Related to Figure 4.

SWF: short-winged female, SWM: short-winged male, LWF: long-winged female, LWM: long-winged male. Scale bar = 500 μm.

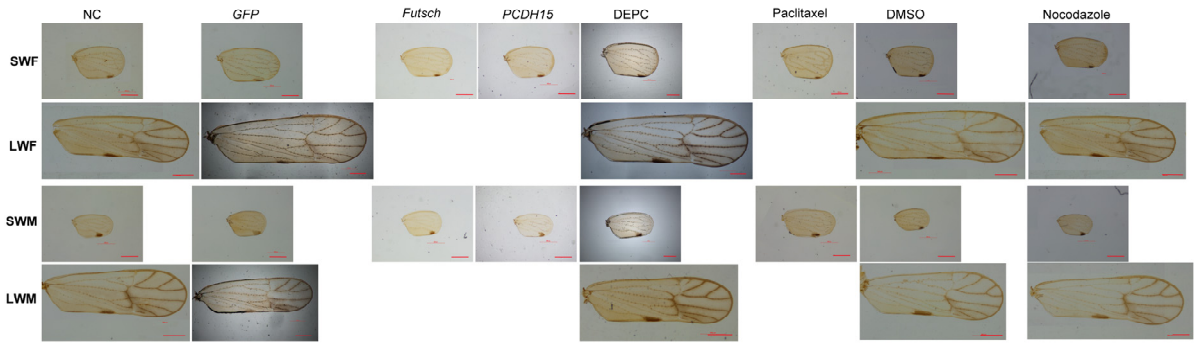

Figure S2: Representative long and short wings after treatment at the 5th instar nymph stage, Related to Figure 5.

SWF: short-winged female, SWM: short-winged male, LWF: long-winged female, LWM: long-winged male. Scale bar = 500 μm.

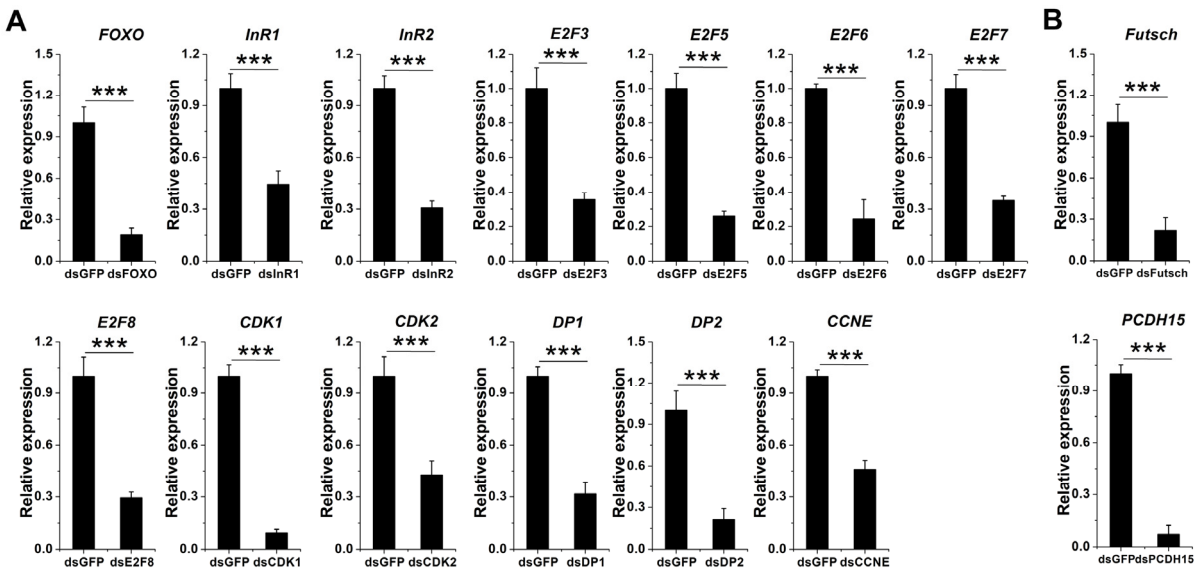

Figure S3: Relative expression of genes down-regulated by RNAi, Related to Figure 4 , 5 and 6.

dsRNA of *InR1*, *InR2* and *FOXO*, *E2F3*, *E2F5*, *E2F6*, *E2F7*, *E2F8*, *CDK1*, *CDK2*, *DP1*, *DP2* and *CCNE* were injected into 4th instar nymphs (A) and dsRNA of *PCDH15* and *Futsch* were injected into the 5th instar nymphs (B). Relative abundance of each transcript three days after dsRNA injection was compared with that from control nymphs injected with GFP dsRNA. Twelve biological replicates were used for each treatment. Bars represent means of three separate measurements. Student's *t*-test was used for statistical comparison. *: P<0.05, **: P<-0.01, ***: P<0.001. The primers for RT-PCR were listed in Table S3.

Table S1: Primers for cloning, Related to Figure 1, 2, 4, 5, 6 and 7.

Name	Sequence (5'-3')	GenBank Accession Number
E2F3F	CACCTCTCCTACAAGTGCAC	XM_022345983.1
E2F3R	CAAGGCCACTGAGAGGAATC	
E2F5F	GTGCTTGAAGGAATCGGTCT	MT240933
E2F5R	TCTTCTGCGCAAACTCAGTT	
E2F6F	GTGCCAATCGAGTCCACATC	MT240934
E2F6R	TCCTGTGGACTATCAGCAGC	
E2F7F	AGACAGGCTCTTCGAGATCT	XM_022328840.1
E2F7R	CAACCCCAATAACTCGAGCA	
E2F8F	TCATTCCTAACCCACCATCCA	XR_002606046.1
E2F8R	ATGAATGATGGGTGGGTGGA	
DP1F	GACTCCTGCCAACAACCAAG	XM_022342425.1
DP1R	TTCCTGCACCGAGTTTGTTG	
DP2F	CACAGCGCCTTCATGATCTC	MT240935
DP2R	CATCGTCGGAGTAGTCGTGA	
CDK1F	GCTTGAGAAGATCGGTGAGG	XM_022336874.1
CDK1R	AACACCCGAGCAATACTTCG	
CDK2F	TACCGCGCGCCTGAGATA	XM_022351965.1
CDK2R	GGGAATAGCGGCTTGTAATCC	
CCNEF	GGACGAGACCTTCTACGAGG	XM_022344075.1
CCNER	CATTGCAGGCTCCATCAGTC	
FutF	GCAGTGTCAAGAGTTGGTCG	XM_022348003.1
FutR	CTCTCTGGTTCCTGTGCAGA	
PCDH15F	GCCATTGATGCTGATGAGGG	MT240936
PCDH15R	CAGTGTGATCGGTCTGGGTA	

FOXOF	CTGTTCCCTGAATCGCCGCT	KM250122
FOXOR	CGTTGCAGTCGAATCCGTCG	
InR1F	GCAGTGGCTCAACAACAAGA	KF974333.1
InR1R	CCTCGCTGAAGAAGTCCAAC	
InR2F	GGAGCTATGGTGTTGTCTTGTG	XM_022333236
InR2R	CTTGAGTTGGCCTCATTGGT	

Table S2: Primers for dsRNA synthesis, Related to 1, 2, 4, 5, 6 and 7.

Name	Sequence (5'-3')
dsE2F3F	TAATACGACTCACTATAGGGAGACCACCACCTCTCCTACAAGTGCAC
dsE2F3R	TAATACGACTCACTATAGGGAGACCACCAAGGCCACTGAGAGGAATC
dsE2F5F	TAATACGACTCACTATAGGGAGACCACGTGCTTGAAATCGGTCT
dsE2F5R	TAATACGACTCACTATAGGGAGACCACTCTTCTGCGCAAACTCAGTT
dsE2F6F	TAATACGACTCACTATAGGGAGACCACGTGCCAATCGAGTCCACATC
dsE2F6R	TAATACGACTCACTATAGGGAGACCACTCCTGTGGACTATCAGCAGC
dsE2F7F	TAATACGACTCACTATAGGGAGACCACAGACAGGCTCTTCGAGATCT
dsE2F7R	TAATACGACTCACTATAGGGAGACCACCAACCCCAATAACTCGAGCA
dsE2F8F	TAATACGACTCACTATAGGGAGACCACTCATTCCTAACCCACCATCCA
dsE2F8R	TAATACGACTCACTATAGGGAGACCACATGAATGATGGGTGGGTGGA
dsDP1F	TAATACGACTCACTATAGGGAGACCACGACTCCTGCCAACAACCAAG
dsDP1R	TAATACGACTCACTATAGGGAGACCACTTCCTGCACCGAGTTTGTTG
dsDP2F	TAATACGACTCACTATAGGGAGACCACCACAGCGCCTTCATGATCTC
dsDP2R	TAATACGACTCACTATAGGGAGACCACCATCGTCGGAGTAGTCGTGA
dsCDK1F	TAATACGACTCACTATAGGGAGACCACGCTTGAGAAGATCGGTGAGG
dsCDK1R	TAATACGACTCACTATAGGGAGACCACAACACCCGAGCAATACTTCG
dsCDK2F	TAATACGACTCACTATAGGGAGACCACGGACGAGACCTTCTACGAGG
dsCDK2R	TAATACGACTCACTATAGGGAGACCACCATTGCAGGCTCCATCAGTC
dsCCNEF	TAATACGACTCACTATAGGGAGACCACTACCGCGCGCCTGAGATA
dsCCNER	TAATACGACTCACTATAGGGAGACCACGGGAATAGCGGCTTGTAATCC
dsFutF	TAATACGACTCACTATAGGGAGACCACGCAGTGTCAAGAGTTGGTCG
dsFutR	TAATACGACTCACTATAGGGAGACCACCTCTCTGGTTCCTGTGCAGA
dsPCDH15F	TAATACGACTCACTATAGGGAGACCACGCCATTGATGCTGATGAGGG
dsPCDH15R	TAATACGACTCACTATAGGGAGACCACCAGTGTGATCGGTCTGGGTA
dsFOXOF	TAATACGACTCACTATAGGGAGACCACCTGTTCCCTGAATCGCCGCT

dsFOXOR	TAATACGACTCACTATAGGGAGACCACCGTTGCAGTCGAATCCGTCG
dsInR1F	TAATACGACTCACTATAGGGAGACCACGCAGTGGCTCAACAACAAGA
dsInR1R	TAATACGACTCACTATAGGGAGACCACCCTCGCTGAAGAAGTCCAAC
dsInR2F	TAATACGACTCACTATAGGGAGACCACGGAGCTATGGTGTTGTCTTGTG
dsInR2R	TAATACGACTCACTATAGGGAGACCACCTTGAGTTGGCCTCATTGGT
dsGFPF	TAATACGACTCACTATAGGGAGACCACTTTGTATAGTTCATCCATGCCATGT
dsGFPR	TAATACGACTCACTATAGGGAGACCACATGAGTAAAGGAGAAGAACTTTTCA

Table S3: Primers for RT-PCR, Related to Figure 7 and S3.

Name	Sequence (5'-3')	Size (bp)
E2F3QF	CCGAGCTGCTCTTCATGTT	95
E2F3QR	AAATGTGCCAATCGAGTCCA	
E2F5QF	CCTGCCGACGACATCAATAT	105
E2F5QR	TCTTTTCGACTTTTCCGCCT	
E2F6QF	TCTAAGATGGGAGGCCAAGT	105
E2F6QR	ATTCCTCTCAGTGGCCTTGA	
E2F7QF	CGTCAATCACAAGGGACACA	105
E2F7QR	GGCTGTTTTGCTGATGAGATG	
E2F8QF	ACATGTCTGCTATTCCCCAAC	103
E2F8QR	ATGAAACGTTGTGGAGGGTG	
DP1QF	TGCTGATGAGTTGGTCGAAG	97
DP1QR	TGCATCGTACACCCTTCTTC	
DP2QF	CTGATTGCCGAGGAAGTGAG	98
DP2QR	TCGTCGGAGTAGTCGTGAG	
CDK1QF	CAAGATTCTCAGCACACCGA	102
CDK1QR	TGATTGAGAGTGTTGGTGGTC	
CDK2QF	TGTCGAATCGCAAACCTCTT	96
CDK2QR	GCCAAGTCGTTTCATCAGGA	
CCNEQF	GTTCGTGAGGTTGGTTCAGT	95
CCNEQR	GGTAGACACAAGTAGCTGCC	
FutQF	AAGCAGCAAAGTGTGGAGAA	99
FutQR	CTTGGCAGCTGTCACTTTTG	
PCDH15QF	CTTATGAGTTTGTGGTGCGC	102
PCDH15QR	ACACTTCGGCATTGATACCC	

FOXOQF	ACCGGTTCATGCGCGTACAG	96
FOXOQR	CTCGACGGCGAGCTGATTTG	
InR1QF	GTCGGAGGAGATCAGCAGTC	101
InR1QR	CCACGTCTCTGTGCACGTAT	
InR2QF	GGAGCTATGGTGTTGTCTTG	97
InR2QR	CCTGCAAGTACGTAGGCTAA	
RPS15QF	TAAAAATGGCAGACGAAGAGCCCAA	150
RPS15QR	TTCCACGGTTGAAACGTCTGCG	

Table S4: Shapiro-Wilk normality test（P-value）, Related to Figure 7.

Gene Template	*CCNE*	*CDK1*	*CDK2*	*DP1*	*DP2*	*E2F3*	*E2F5*	*E2F6*	*E2F7*	*E2F8*	*FOXO*	*InR1*	*InR2*	*Futsch*	*PCDH15*
dsGFP	0.468	0.96	0.353	0.102	0.957	0.633	0.214	0.278	0.369	0.353	0.831	0.643	0.294	0.741	0.875
dsCCNE	0.149														
dsCDK1		0.298													
dsCDK2			0.492												
dsDP1				0.082											
dsDP2					0.27										
dsE2F3						0.361									
dsE2F5							0.468								
dsE2F6								0.313							
dsE2F7									0.181						
dsE2F8										0.31					
dsFOXO											0.89				
dsInR1												0.084			
dsInR2													0.603		
dsFutsch														0.401	
dsPCDH15															0.114

Table S5: Shapiro-Wilk normality test（P-value）, Related to Figure 7.

Gene / Template	*CCNE*	*CDK1*	*CDK2*	*DP1*	*DP2*	*E2F3*	*E2F5*	*E2F6*	*E2F7*	*E2F8*	*Futsch*	*PCDH15*
dsGFP+H_2O	0.975	0.08	0.505	0.604	0.808	0.294	0.998	0.578	0.124	0.502	0.078	0.391
dsGFP+PTX	0.405	0.632	0.935	0.883	0.447	0.929	0.183	0.615	0.799	0.09	0.122	0.669
dsFOXO+H_2O	0.191	0.053	0.136	0.216	0.574	0.871	0.814	0.194	0.286	0.664	0.544	0.158
dsFOXO+PTX	0.986	0.35	0.423	0.893	0.285	0.216	0.887	0.125	0.38	0.104	0.074	0.269

Transparent Methods

Insect rearing

Brown planthoppers were maintained in the lab and were originally a gift of Z.R. Zhu (Institute of Insect Science, Zhejiang University, China). The long- and short-winged adults were classified based on wing morphology as previously reported (Lin et al., 2016a; Lin et al., 2016b; Lin et al., 2016c). Seedlings of rice variety IIyou-023 (*Oryza sativa* L. cv.) cultured with nutrient solution (Yoshida et al., 1976) were used to feed the insects. Insects were maintained at 28℃, light:dark = 14h:10h, 70%-80% humidity.

Wing-bud dissection and staining

Brown planthopper nymphs were developmentally staged and collected. Wing pads were dissected in cold (4°C) PBS. Dissected wing pads were then fixed in 4% paraformaldehyde in PBS (Sangon Biotech, Shanghai, China) and washed three times in PBS (15 min./wash). For visualization of the nucleus, DAPI (1:1000, Sangon Biotech, Shanghai, China) was used. Phalloidin-iFluor 488 (1:100, Abcam, USA) was used for visualization of the actin cytoskeleton. Samples were incubated with stain for 1 hour at room temperature, then washed four times in PBS (15 min./wash) and mounted on slides in Anti-Fade Mounting Medium (Sangon Biotech, Shanghai, China).

Light Microscopy

A Zeiss confocal microscope (Zeiss LSM800, Zeiss, Germany) was used to visualize nuclei (DAPI) and actin cytoskeletons (Phalloidin-iFluor 488, Abcam, USA) of the wing pads. The distal region of the wing-pads was imaged. Images were acquired using Axion Vision and were processed using Adobe Photoshop 10.

Transmission Electron Microscopy (TEM)

Dissected wing-pads were fixed in 2.5% glutaraldehyde for 12 h，rinsed with 0.1M PBS (pH7) 3 times for 15 min each，fixed in 1% osmium tetroxide for 1.5 h, then rinsed twice in PBS (15 min each). Wing pads were then sequentially dehydrated with 50%, 70%, 80%, 90%, 95% ethanol, 15min each wash, 100% ethanol for 20 min and then 100% acetone for 20 min. The sample was treated with embedding agent and acetone at a volume ratio of 3:1 for 1 h, followed by a volume ratio of 1:1 for 3 h, and then with pure embedding agent for 12 h. The sample was placed in a heating polymerization apparatus at 70° C for 48 h, the excess resin was removed, and the sample was sliced using a Leica EM UC7 slicer, to a thickness of 70nm per slice. Slices were stained using uranyl acetate 50% ethanol saturated solution for 1 h, double distilled water elution, citric acid lead staining for 15 min, and the sample was observed using a Hitachi H-7650 electron microscopic.

Cloning of genes for dsRNA synthesis

Total RNA was extracted using the Trizol-based RNAiso Plus total RNA extraction kit (Takara, Dalian, China), and the Roche Transcriptor First Strand cDNA synthesis kit (Roche Applied Science, Shanghai, China) was used to synthesize first strand cDNA. Sequences of *NlInR1*, *NlInR2* and *NlFOXO* were identified from previously published *N. lugens* sequences (Lin et al., 2016b; Lin et al., 2016c; Xu et al., 2015). The previously cloned *InR1* and *FOXO* DNA fragments used as templates for dsRNA synthesis were amplified by PCR using

Ex-Taq polymerase (Takara, Dalian, China). *E2F3*, *E2F5*, *E2F6*, *E2F7*, *E2F8*, *CDK1*, *CDK2*, *DP1*, *DP2* *CCNE*, *Futsch* and *PCDH15* were identified from the transcriptome sequence (Xue et al., 2010) and the NCBI database (www.ncbi.nlm.nih.gov). All the primers are listed in Table S1. Genes were then cloned, confirmed by sequencing, and used as template for double stranded RNA (dsRNA) synthesis.

Injection of dsRNA and chemical inhibitors

RiboMAX™ Large Scale RNA Production System-T7 (Promega, Beijing, China) was used to synthesize dsRNA. dsRNAs of *InR1*, *FOXO*, *E2F3*, *E2F5*, *E2F6*, *E2F7*, *E2F8*, *CDK1*, *CDK2*, *DP1*, *DP2* and *CCNE*, were synthesized. The procedure was the same as described in Technical Bulletin TB166 (Promega, Beijing, China) except different templates were used to synthesize dsRNAs and different dsRNA primers (with a 27-base T7 sequence at the 5' end, Table S2) were used. Nocodazole (0.1 mM, dissolved in DMSO, MedChem Express, Shanghai, China) and Paclitaxel (0.1 mM, dissolved in DEPC-treated water, Sangon Biotech, Shanghai, China) were injected into 5^{th} instar nymphs in a total volume of 0.l μl per nymph. 4^{th} and 5^{th} instar brown planthopper nymphs were anesthetized by CO_2 before injection. A Nikon microscope and Narishige injection system (MN-151, Narishige) were used for injection and the procedure was the same as previously described (Lin et al., 2014). Each nymph was injected with 0.1 μg dsRNA, and afterwards the nymphs were allowed to recover for 2 hours before being returned to rice seedlings.

RT-PCR

Total RNA was isolated from dissected wing pads as above. 12 biological replicates were used for each treatment and twenty brown planthoppers were pooled for each replicate. Three technical replicates were used for each biological replicate and were averaged for statistical analysis. Smple sizes were indicated in the figure legend. Roche SYBR® Green PCR Master Mix and SYBR® Green RT-PCR Reagents kits (Roche Applied Science, Shanghai, China) were used for RT-PCR and first-strand cDNA synthesis, which was diluted 20 times after synthesis. For the first strand cDNA synthesis, we used 25 μl reaction, and 2 μl of diluted cDNA was used as template. Roche SYBR® Green PCR Master Mix and SYBR® Green RT-PCR Reagents kits (Roche Applied Science, Shanghai, China) were used for RT-PCR and first-strand cDNA synthesis, which was diluted 20 times after synthesis. For the first srand cDNA synthesis, we used 25 μl reaction, and 2 μl of diluted cDNA was used as template. $2^{-\Delta\Delta Ct}$ relative expression method was used for the expression level comparison (Livak and Schmittgen, 2001). The reference gene (*RPS15*) used was selected according to a previous study (Yuan et al., 2014). The primers used are shown in Table S3.

Measuring the number of nuclei

Image J (National Institutes of Health, USA) was used for nuclei number counting. The area was delineated, which was 475 μm^2 per block. The number of blocks used was not less than 9. The images were transformed into 8-bit TIFF format, i.e., the color picture was changed into black and white.

Flow cytometry

Wings were removed from newly emerged brown planthopper adults and placed in a 1.5 mL centrifuge tube in PBS. The wings were ground with a pestle. The ground samples were centrifuged (10000 g, 4°C, 3 min), the supernatant was discarded, the samples were resuspended in ethanol (100%) and placed on ice for 1 h, and then centrifuged (10000 g, 3 min, 4°C), the supernatant was discarded, the samples were resuspended in 1X PBS plus 0.25% Triton, and then held at 4°C for 10 min. The sample was centrifuged (10000g, 3min), the supernatant was discarded, and DAPI (1:1000, Sigma Aldrich, Shanghai, China) was then added. Samples were then measure in a Beckman CytoFLEX flow cytometer. Cell cycle analysis was carried out using FlowJo (FlowJo, LLC, USA).

Statistical analysis

SPSS 20.0 was used for statistical analyses. Chi-square test was used for comparison of the wing-morph ratios after treatment with dsRNAs. For independent sample t test, we first analyzed whether the data was normally distributed. Then independent sample t tests were carried out.

For one-way ANOVA, we first checked that the data of each group was normally distributed (Table S4, S5). Then ANOVA was carried out, and multiple comparison methods were selected based on the homogeneity test results. If the variance was homogeneous, we selected the LSD method under "Assumed Homogeneity of Variance" in the multiple comparisons; if the variance was not homogeneous, we selected Dunnett's T3 under "Unhypothesized Homogeneity of Variance". Different letters indicate significant differences ($P<0.01$).

Supplemental References

Lin, X., Xu, Y., Yao, Y., Wang, B., Lavine, M.D., and Lavine, L.C. (2016a). JNK signaling mediates wing form polymorphism in brown planthoppers (Nilaparvata lugens). Insect Biochem Mol Biol *73*, 55-61.

Lin, X., Yao, Y., Jin, M., and Li, Q. (2014). Characterization of the Distal-less gene homologue, NlDll, in the brown planthopper, Nilaparvata lugens (Stal). Gene *535*, 112-118.

Lin, X., Yao, Y., Wang, B., Emlen, D.J., and Lavine, L.C. (2016b). Ecological Trade-offs between Migration and Reproduction Are Mediated by the Nutrition-Sensitive Insulin-Signaling Pathway. Int J Biol Sci *12*, 607-616.

Lin, X., Yao, Y., Wang, B., Lavine, M.D., and Lavine, L.C. (2016c). FOXO links wing form polyphenism and wound healing in the brown planthopper, Nilaparvata lugens. Insect Biochem Mol Biol *70*, 24-31.

Livak, K.J., and Schmittgen, T.D. (2001). Analysis of relative gene expression data using real-time quantitative PCR and the 2(-Delta Delta C(T)) Method. Methods *25*, 402-408.

Xu, H.J., Xue, J., Lu, B., Zhang, X.C., Zhuo, J.C., He, S.F., Ma, X.F., Jiang, Y.Q., Fan, H.W., Xu, J.Y.*, et al.* (2015). Two insulin receptors determine alternative wing morphs in planthoppers. Nature *519*, 464-467.

Xue, J., Bao, Y.-Y., Li, B.-l., Cheng, Y.-B., Peng, Z.-Y., Liu, H., Xu, H.-J., Zhu, Z.-R., Lou, Y.-G., Cheng, J.-A.*, et al.* (2010). Transcriptome Analysis of the Brown Planthopper Nilaparvata lugens. PLoS One *5*, e14233.

Yoshida, S., Forno, D.A., and Cock, J.H. (1976). Laboratory manual for physiological studies of rice (International Rice Research Institute).

Yuan, M., Lu, Y., Zhu, X., Wan, H., Shakeel, M., Zhan, S., Jin, B.R., and Li, J. (2014). Selection and evaluation of potential reference genes for gene expression analysis in the brown planthopper, Nilaparvata lugens (Hemiptera: Delphacidae) using reverse-transcription quantitative PCR. PLoS One *9*, e86503.